Nonlinear Dyn (2014) 78:147–161
DOI 10.1007/s11071-014-1428-8

ORIGINAL PAPER

Dynamic delayed feedback control for stabilizing the giant swing motions of an underactuated three-link gymnastic robot

Dasheng Liu · Guozheng Yan · Hiroshi Yamaura

Received: 6 October 2012 / Accepted: 21 April 2014 / Published online: 28 May 2014

Abstract This paper investigates the dynamics of the giant swing motions of an underactuated three-link gymnastic robot moving in a vertical plane by means of dynamic delayed feedback control (DDFC). DDFC, being one of useful methods to overcome the so-called odd number limitation in controlling a chaotic discrete-time system, is extended to control a continuous-time system such as a 3-link gymnastic robot with passive joint. Meanwhile, a way to calculate the error transfer matrix and the input matrix which are necessary for discretization is proposed, based on a Poincaré section which is defined to regard the target system as a discrete-time system. Moreover, the stability of the closed-loop system by the proposed control strategy is discussed. Furthermore, some numerical simulations are presented to show the effectiveness in controlling a chaotic motion of the 3-link gymnastic robot to a periodic giant swing motion.

Keywords Dynamic delayed feedback control · Chaos control · Gymnastic robot · Nonholonomic system · Giant swing motion · Stabilization

D. Liu (✉)
Institute of Medical Precision Engineering and Intelligent System, School of Electronic Information and Electrical Engineering, Shanghai JiaoTong University, Shanghai 200240, China
e-mail:dsliu@sjtu.edu.cn

G. Yan
School of Electronic Information and Electrical Engineering, Shanghai JiaoTong University, Shanghai 200240, China
e-mail:gzhyan@sjtu.edu.cn

H. Yamaura
Graduate School of Science and Engineering, Tokyo Institute of Technology, 2-12-1-I3-10, Ookayama, Meguro-ku, Tokyo 152-8552, Japan
e-mail:yamaura@mech.titech.ac.jp

1 Introduction

Underactuated mechanical systems, such as surface vessels, underwater vehicles, helicopters, road vehicles, underactuated manipulators, flexible joint and flexible link robots, space robots, mobile robots, and acrobat, refer to the systems possessing less number of actuators than degrees of freedom. These systems generate interesting control problems which require fundamental nonlinear approaches. Such systems exhibit often complex internal dynamics, nonholonomic behavior, and lack of feedback linearizability, which make the class a rich one from a control standpoint.

The gymnastic robot, whose first joint is passive and the rest are active, is classified as an underactuated robot [1]. Open-loop dynamic characteristics of such a linkage as this kind of system with nonholonomic constraints, shows the chaotic nature that small differences in initial conditions yield widely diverging outcomes for its nonlinearity due to centrifugal force, coriolis force, and gravity. In the past few years, the research in this area has made great progress [2–9].

However, a generalized control method has not yet been established to this kind of system for the difficulties in analysis, their control problems remain challenging.

The giant swing motions existing in the gymnastic robot are, needless to say, a kind of periodic motion. Meanwhile, each motion such as bipedal locomotion of walking robot [10], swing and locomotion of brachiation robot [11], can also be considered as a special kind of periodic one which is achieved by repeating a half-cycle movement. However, the characteristic of the periodic motion of these underactuated systems has not been understood clearly. As is known that the classical and the most frequently used tool for analysis of existence and stability of periodic trajectories of nonlinear dynamical systems is the Poincaré first-return map, which is defined on a hyper-surface transversal to dynamics at a point of the cycle. Calculation of the Poincaré map of a nonlinear system typically cannot be done analytically and requires numerical solution of the system dynamics for a large number of initial conditions. It is often computationally expensive and of limited use, if one look for periodic solutions which are open-loop unstable, or if one look for design of a stabilizing controller. This motivates investigation of alternative strategies.

On the other hand, in 1990, Ott et al. [12] pointed out that the existence of many unstable periodic orbits (UPOs) embedded in chaotic attractors raises the possibility of using very small external forces to obtain various types of regular behavior. Since then, study on dynamics and control of chaotic phenomena in deterministic nonlinear dynamical systems had attracted increasing attention. In order to improve the performance of the characteristics of the system or avoid the chaotic phenomena, it is required to control a chaotic system to a periodic motion which is beneficial for working with a particular condition. For this purpose, many control methods such as time delay feedback control [13–15], robust control [16], adaptive control [17,18], sliding mode control [19,20], fuzzy adaptive sliding mode control [21], back-stepping design [22], intermittent control [23,24], etc., have been proposed to control chaos. Among them, the delayed feedback control (DFC) has gained widespread acceptance. DFC involves a control input formed from the difference between the current state of the system and the state of the system delayed by one period of the UPOso that the control signal vanishes when the stabilization of a periodic orbit is attained.

Nevertheless, some general analytical results have proved that the DFC has a limitation that if the linear variational equation about the target UPO has an odd number of real characteristic multipliers greater than unity, the UPO can never be stabilized with any value of feedback gain. This statement was first proved by Ushio [25] for discrete-time systems. Just et al. [26] and Nakajima [27] proved the same limitation for the continuous-time DFC. Since then, several modifications [28–38] of the original DFC method have been proposed in order to improve its performance. However, in applying the DFC to the continuous system, stability analysis of the closed-loop system is very difficult since the time-delay dynamics described by a difference-differential equation takes place in infinite dimensional phase spaces. In order to overcome this difficulty, the authors have proposed some control strategies such as prediction-based delayed feedback control (PDFC) [39], multiple-prediction delayed feedback control (MPDFC) [40,41], for stabilizing the unstable periodic orbits embedded in the giant swing motions of the gymnastic robot. Although it has been shown that PDFC is effective in the control of the giant swing motions, it has a deficiency that needs to predict the movement state of future one period. Therefore, it is necessary to try some other modified methods based on DFC to improve the effectiveness of controlling the giant swing motions. In the further research, a method named as extended dynamic delayed feedback control (EDDFC), which is an extension of the original dynamic DFC [28] designed for a discrete-time system, proposed to control the giant swing motion of an underactuated 3-link gymnastic robot.

This paper is organized as follows: Section 2 gives briefly the mathematical model of the 3-link gymnastic robot. Section 3 demonstrates the complex dynamics relevant to periodic and chaotic motions of the free giant swing motions of the gymnastic robot with different initial conditions. Section 4 discusses in detail a strategy for stabilizing the periodic motions embedded in a continuous-time system, such as a 3-link gymnastic robot by the EDDFC method. In Sect. 5, some numerical simulations show the effectiveness of the proposed method. Section 6 summarizes the paper.

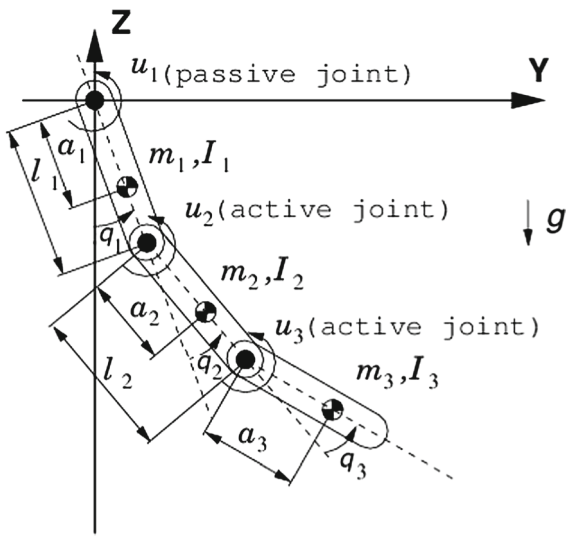

Fig. 1 3-DOF gymnastic robot model

2 Model of a 3-link gymnastic robot

The 3-link gymnastic robot is a simplified model of a human gymnast on a high bar, where the underactuated first joint models the gymnast's hands on the bar, the rest two actuated joints model, respectively, the gymnast's shoulders (joint 2) and hips (joint 3). As shown in Fig. 1, for the ith ($i = 1, 2, 3$) link, m_i is its mass, l_i is its length, a_i is the distance from joint i to its center of mass, I_i is the inertia moment around its center of mass, and g denotes the acceleration of gravity.

The equation of motion of the gymnastic robot can be described as the following equation [40].

$$\begin{bmatrix} u_1 \\ u_2 \\ u_3 \end{bmatrix} = \begin{bmatrix} M_{11} & M_{12} & M_{13} \\ M_{21} & M_{22} & M_{23} \\ M_{31} & M_{32} & M_{33} \end{bmatrix} \begin{bmatrix} \ddot{q}_1 \\ \ddot{q}_2 \\ \ddot{q}_3 \end{bmatrix} + \begin{bmatrix} C_1 \\ C_2 \\ C_3 \end{bmatrix} + \begin{bmatrix} G_1 \\ G_2 \\ G_3 \end{bmatrix} \tag{1}$$

Here, $q = (q_1, q_2, q_3)^{\mathrm{T}} \in \Re^3$ is the generalized coordinate vector, $(u_1, u_2, u_3)^{\mathrm{T}} \in \Re^3$ is the joint torque vector, and $M_{i,j}, C_i, G_i (i = 1, 2, 3; j = 1, 2, 3)$ denote the items of the inertia matrix, Coriolis matrix, gravitational matrix, respectively.

In addition, since the first joint cannot generate active torque, the following constraint must be satisfied.

$$u_1 \equiv h(\ddot{q}, \dot{q}, q) = 0 \tag{2}$$

In order to facilitate the analysis, Eq. (1) is rewritten into the following equation.

$$\begin{bmatrix} \dot{q} \\ \ddot{q} \end{bmatrix} = \begin{bmatrix} \dot{q} \\ -M^{-1}(q)(C(q, \dot{q}) + G(q)) \end{bmatrix} + \begin{bmatrix} 0 \\ M^{-1}(q)E \end{bmatrix} \begin{bmatrix} u_2 \\ u_3 \end{bmatrix}, \tag{3}$$

where

$$\begin{aligned} M(q) &= [M_1(q), M_2(q), M_3(q)]^T, \\ M_1(q) &= [r_1 + r_2 + r_3 + 2(s_1 + s_2)\cos q_2 + 2s_3 \cos q_3 \\ &\quad + 2s_4 \cos(q_2 + q_3), r_2 + r_3 + (s_1 + s_2)\cos q_2 \\ &\quad + 2s_3 \cos q_3 + s_4 \cos(q_2 + q_3), r_3 + s_3 \cos q_3 \\ &\quad + s_4 \cos(q_2 + q_3)], \\ M_2(q) &= [r_2 + r_3 + (s_1 + s_2)\cos q_2 + 2s_3 \cos q_3 \\ &\quad + s_4 \cos(q_2 + q_3), r_2 + r_3 + 2s_3 \cos q_3, r_3 \\ &\quad + s_3 \cos q_3], \\ M_3(q) &= [r_3 + s_3 \cos q_3 + s_4 \cos(q_2 + q_3), r_3 \\ &\quad + s_3 \cos q_3, r_3], \end{aligned}$$

and

$$\begin{aligned} C(x) &= [C_1(q, \dot{q}), C_2(q, \dot{q}), C_3(q, \dot{q})]^T, \\ C_1(q, \dot{q}) &= -(2\dot{q}_1\dot{q}_2 + \dot{q}_2^2)(s_1 + s_2)\sin q_2 - (2\dot{q}_1\dot{q}_3 \\ &\quad + 2\dot{q}_2\dot{q}_3 + \dot{q}_3^2)s_3 \sin q_3 - (\dot{q}_2^2 + \dot{q}_3^2 \\ &\quad + 2\dot{q}_1\dot{q}_2 + 2\dot{q}_2\dot{q}_3 + 2\dot{q}_1\dot{q}_3)s_4 \sin(q_2 + q_3), \\ C_2(q, \dot{q}) &= \dot{q}_1^2 \{(s_1 + s_2)\sin q_2 + s_4 \sin(q_2 + q_3)\} \\ &\quad - (2\dot{q}_1\dot{q}_3 + 2\dot{q}_2\dot{q}_3 + \dot{q}_3^2)s_3 \sin q_3, \\ C_3(q, \dot{q}) &= \dot{q}_1^2 \{s_4 \sin(q_2 + q_3) + s_3 \sin q_3\} \\ &\quad + (2\dot{q}_1\dot{q}_2 + \dot{q}_2^2)s_3 \sin q_3, \end{aligned}$$

and

$$\begin{aligned} G(q) &= [G_1(q), G_2(q), G_3(q)]^T, \\ G_1(q) &= g_1 \sin q_1 + g_2 \sin(q_1 + q_2) \\ &\quad + g_3 \sin(q_1 + q_2 + q_3), \\ G_2(q) &= g_2 \sin(q_1 + q_2) + g_3 \sin(q_1 + q_2 + q_3), \\ G_3(q) &= g_3 \sin(q_1 + q_2 + q_3), \end{aligned}$$

and

$$E = \begin{bmatrix} 0 & 0 \\ 1 & 0 \\ 0 & 1 \end{bmatrix}.$$

The variables among the above equation is defined as follows:

$$r_1 = I_1 + m_1 a_1^2 + m_2 l_1^2 + m_3 l_1^2,$$

$$
\begin{aligned}
r_2 &= I_2 + m_2 a_2^2 + m_3 l_2^2,\\
r_3 &= I_3 + m_3 a_3^2,\\
s_1 &= m_2 l_1 a_2,\\
s_2 &= m_3 l_1 l_2,\\
s_3 &= m_3 l_2 a_3,\\
s_4 &= m_3 l_1 a_3,\\
g_1 &= g\left\{m_1 a_1 + (m_2 + m_3) l_1\right\},\\
g_2 &= g(m_2 a_2 + m_3 l_2),\\
g_3 &= g m_3 a_3.
\end{aligned}
$$

3 Dynamics of a 3-link gymnastic robot

The differential equation (1) cannot be analytically integrated, except for a special case of link parameters, since it contains the so-called nonholonomic constraints. The past researches have shown that this kind of system displays a chaotic motion if no control input.

In the gymnastic robot model (3), the conditions of a periodic giant swing motion can be represented as boundary conditions of one revolution movement as follows:

$$
\begin{aligned}
&q_1(0) = -\pi, q_1(T) = \pi, \quad \dot{q}_1(0) = \dot{q}_1(T),\\
&q_2(0) = q_2(T) = 0, \quad \dot{q}_2(0) = \dot{q}_2(T),\\
&q_3(0) = q_3(T) = 0, \quad \dot{q}_3(0) = \dot{q}_3(T),
\end{aligned} \tag{4}
$$

where T is the period of movement.

Thus, the initial value problem of the giant swing motion becomes a boundary value problem. Based on the above-mentioned boundary conditions, an initial condition from which can achieve a free giant swing motion, could be obtained by means of the shooting method. In solving the differential equations (3), 4th-order Runge–Kutta method was used with time step $\mathrm{d}t = 1\,\mathrm{ms}$. See Table 1 for the parameters of the model. The parameters m_i, l_i, a_i are the morphological data provided based on an assumed men with 1.7m height, 60Kg weight, and I_i is calculated on the basis of assumptions that its head and hands are each a solid sphere of constant density, the other segments are each a constant density straight bar [42,43]. In addition, take $g = 9.81[\mathrm{m/s^2}]$.

Table 1 Link parameter values

	1st link	2nd link	3rd link
Mass m_i (kg)	6.06	33.4	20.7
Moment of inertia I_i (kgm^2]	0.193	1.80	1.56
Link length l_i (m)	0.593	0.602	0.879
Offset of mass center a_i (m)	0.299	0.245	0.377

As a classical tool for diagnosing whether or not a system is chaotic, Lyapunov exponents, which provide a qualitative and quantitative characterization for dynamical behavior, are related to the exponentially fast divergence or convergence of nearby orbits in phase space. A system with one or more positive Lyapunov exponents is usually taken as an indication that the system is chaotic. Therefore, Lyapunov exponent was calculated as follows: for the gymnastic robot system (3), using the algorithm given in the reference [44].

$$
\begin{aligned}
&\{\lambda_1, \lambda_2, \lambda_3, \lambda_4, \lambda_5, \lambda_6\} = \{0.0015445, 0.0016542,\\
&\quad 0.0011756, -0.00080229, -0.0017139, -0.0018667\}
\end{aligned}
$$

Since that λ_2, being the largest Lyapunov exponent, is greater than zero, it can be said that the system (3) is chaotic.

In order to conform the detail of the dynamics of the 3-link gymnastic robot, it is enumerated several types of steady states at different initial conditions. Figure 2 depicts the phase portraits which show the dynamics of the system starting from different initial conditions, in which Fig.2a and c shows the dynamics of the system with the initial conditions obtained by the shooting method, while Fig. 2b and d displays that of the system with the initial conditions containing errors. Here, q_i and $\dot{q}_i$ refer to, respectively, the angle, angular velocity of the ith ($i = 1, 2, 3$) link of the gymnastic robot. From Fig. 2, it can be observed that the free giant swing motion of the gymnastic robot is sensitive to initial conditions and displays a chaotic behavior.

4 Dynamic delayed feedback control

4.1 Original dynamic delayed feedback control

In the original dynamic delayed feedback control [28], an nth-order nonlinear discrete-time system described by Eq. (5) is considered.

$$
\mathbf{x}(k+1) = f(\mathbf{x}, u(k)) \tag{5}
$$

where $\mathbf{x} \in \Re^n$ is the state and $u(k) \in \Re^n$ is the input. For simplicity, it is considered the stabilization of an unstable fixed point of the system (5). If define

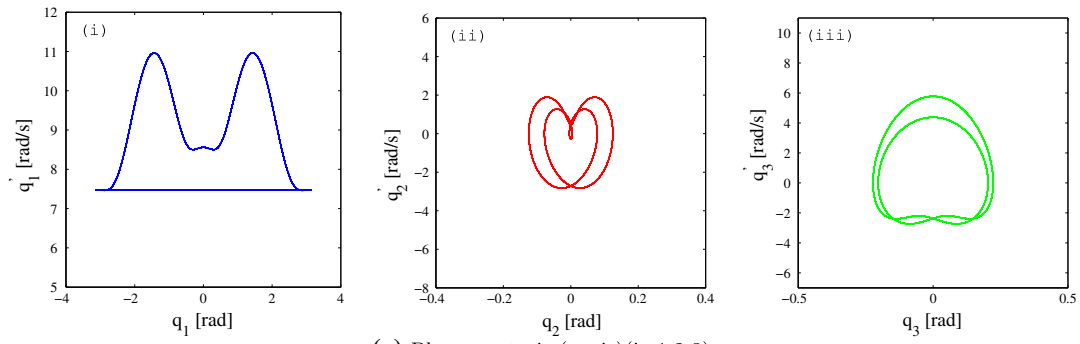

(a) Phase portrait $(q_i, \dot{q}_i)$(i=1,2,3)

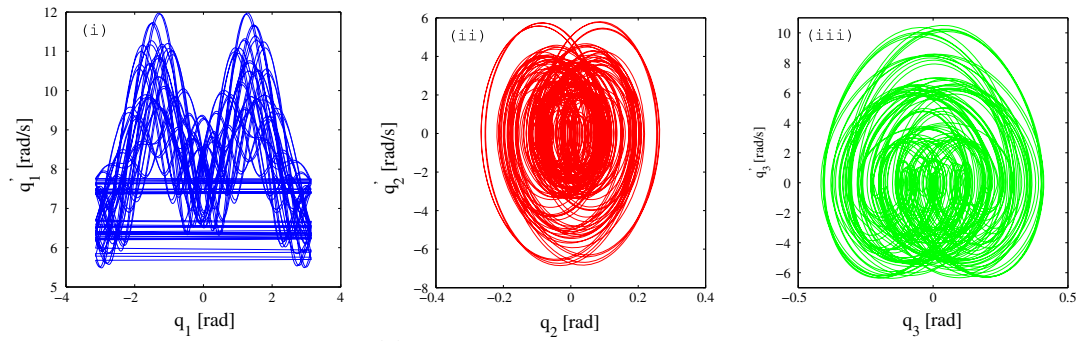

(b) Phase portrait $(q_i, \dot{q}_i)$(i=1,2,3)

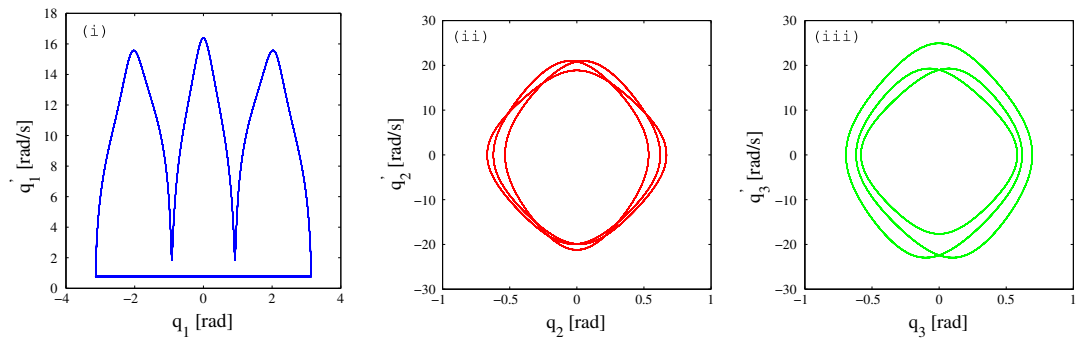

(c) Phase portrait $(q_i \ \dot{q}_i)$(i=1 2 3)

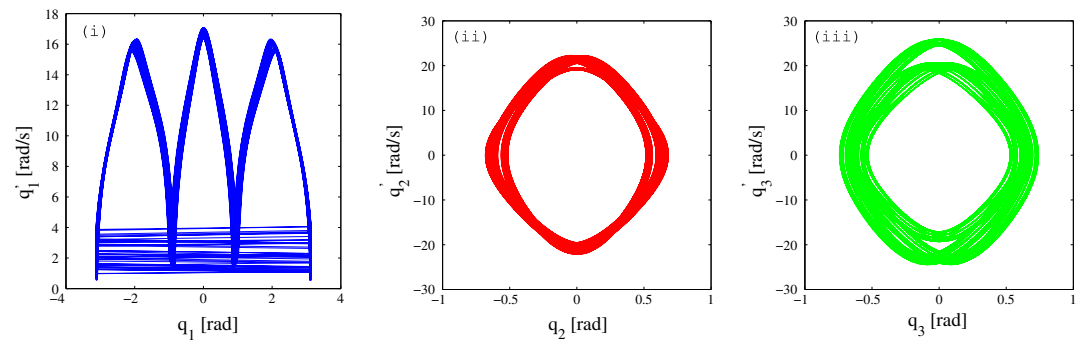

(d) Phase portrait $(q_i, \dot{q}_i)$(i=1,2,3)

Fig. 2 Phase portraits $(q, \dot{q})$ of several types of steady states with different initial conditions: **a** $(-\pi, 0, 0, 7.483, -0.278, 4.383)$, **b** $(-\pi, 0.1, 0.2, 6.683, 0.222, 3.183)$, **c** $(-\pi, 0, 0, 0.763, 18.886, -17.648)$, **d** $(-\pi, 0.05, 0.05, 0.863, 19.292, -18.25)$; q_i and $\dot{q}_i$ refer to, respectively, the angle, angular velocity of the ith $(i = 1, 2, 3)$ link

$\mathbf{x}_f = f(\mathbf{x}_f, 0)$, where $\mathbf{x}_f$ is a fixed point of the system (5) with $u(k) = 0$, then, the linearized system around $\mathbf{x}_f$ is obtained as follows:

$$x(k+1) = Ax(k) + Bu(k). \tag{6}$$

Here,

$$A = \frac{\partial}{\partial \mathbf{x}} f(\mathbf{x}_f, 0) \in \Re^{n\times n}, \quad B = \frac{\partial}{\partial u} f(\mathbf{x}_f, 0) \in \Re^{n\times m}.$$

The original DDFC, which is an $\hat{n}$th-order linear dynamic controller, proposed by Yamamoto et al. is given by

$$\left.\begin{aligned} \hat{x}(k+1) &= \hat{A}\hat{x}(k) + \hat{B}y(k), \\ u(k) &= \hat{C}\hat{x}(k) + \hat{D}y(k), \\ y(k) &= x(k) - x(k-1), \end{aligned}\right\} \tag{7}$$

where $\hat{A} \in \Re^{\hat{n}\times\hat{n}}$, $\hat{B} \in \Re^{\hat{n}\times n}$, $\hat{C} \in \Re^{m\times\hat{n}}$, $\hat{D} \in \Re^{m\times n}$, and $\hat{x} \in \Re^{\hat{n}}$. In addition, $\hat{x}$ is the state of the controller.

4.2 Extended dynamic DFC

Due to the dynamic DFC is proposed for the discrete-time system, it could not be applied directly to the continuous-time system. Therefore, it needs some further processes.

Let $\mathtt{x} = (q, \dot{q})$, the 3-link gymnastic robot model (3) can be described as follows:

$$\dot{\mathtt{x}} = f(\mathtt{x}, \mathtt{u}). \tag{8}$$

Here, assume $f(\cdot)$ is differentiable.

4.2.1 Discretization of the system

It is well known that the stabilization problem of periodic orbits in continuous-time systems such as the underactuated 3-link gymnastic robot can be reduced to the fixed points stabilization problem of discrete-time systems by using a Poincaré map. Note that the periodic motion in state space has the property of passing through the same point per cycle. It is considered to evaluate the stability of the movement by calculating discretely the error between the current motion and the target periodic orbit.

Define the solution of equation passing through $x(0)$ at $t = 0$ as follows:

$$x(0) = x_0. \tag{9}$$

Then, the solutions of Eq. (8) starting from the initial condition $x(0)$ can be described by the following equation:

$$x(t) = \varphi(t, x_0, u_0), \tag{10}$$

where $\varphi(\cdot)$ is the function of x.
Moreover, the periodic solution satisfies

$$x(T) = x(0) = \varphi(T, x_0, u_0). \tag{11}$$

A Poincaré map P is defined as follows:

$$P : \begin{array}{l} R^n \to R^n \\ x_0 \mapsto x_1 = \varphi(T(x_0), x_0, u_0) \end{array} \tag{12}$$

Here, $T(x_0)$ is the time required to meet again in a Poincaré map, P, while trajectory starts from the initial condition, x_0.

Define the intersection point of periodic orbit and Poincaré map be $\bar{x}$, which satisfies the following relationship.

$$\bar{x} = P(\bar{x}, \bar{u}) = \varphi(T(\bar{x}), \bar{x}, \bar{u}) \tag{13}$$

The variation equations around the intersection points, $\bar{x}$, can be described as follows:

$$\left.\begin{aligned} \mathbf{x}(k) &= \bar{x} + x(k), \\ \mathbf{u}(k) &= \bar{u} + u(k), \end{aligned}\right\} \tag{14}$$

where $\mathbf{x}(k)$ means

$$\mathbf{x}(k) = \varphi(T(x(k-1)), x(k-1), u(k-1)).$$

From Eqs. (13) and (14), the following equation is derived.

$$\begin{aligned} \mathbf{x}(k+1) &= \bar{x} + x(k+1) \\ &= P(\bar{x} + x(k), \bar{u} + u(k)) \end{aligned} \tag{15}$$

Using the above equation's Taylor series at $\bar{x}$ and neglecting the higher order terms can yield

$$x(k+1) = Ax(k) + Bu(k), \tag{16}$$

where

$$A = \frac{\partial P}{\partial \bar{x}}, \quad B = \frac{\partial P}{\partial \bar{u}}.$$

Here, k is the discrete time and $x(k) \in \Re^n$, $A \in \Re^{n\times n}$, $B \in \Re^{n\times m}$ denote the state error, the error transfer matrix, and the input matrix in terms with the Poincaré map, respectively.
Substituting Eq. (10) into Eq. (8), one can obtain

$$\frac{\mathrm{d}\varphi(t, x_0, u_0)}{\mathrm{d}t} = f(\varphi(t, x_0, u_0), u). \tag{17}$$

Next, taking differentiation for Eq. (17) at x_0 or u_0, the following equations can be obtained, respectively.

$$\frac{\partial}{\partial x_0}\left(\frac{\mathrm{d}\varphi}{\mathrm{d}t}(t,x_0,u_0)\right)=\frac{\partial f(\varphi(t,x_0,u_0),u)}{\partial x_0} \tag{18}$$

$$\frac{\partial}{\partial u_0}\left(\frac{\mathrm{d}\varphi}{\mathrm{d}t}(t,x_0,u_0)\right)=\frac{\partial f(\varphi(t,x_0,u_0),u)}{\partial u_0} \tag{19}$$

Changing the differential order of the left-hand side in the Eqs. (18) and (19) yields the following equations.

$$\frac{\mathrm{d}}{\mathrm{d}t}\left(\frac{\partial\varphi}{\partial x_0}(t,x_0,u_0)\right)=F_x\frac{\partial\varphi}{\partial x_0}(t,x_0,u_0) \tag{20}$$

$$\frac{\mathrm{d}}{\mathrm{d}t}\left(\frac{\partial\varphi}{\partial u_0}(t,x_0,u_0)\right)=F_x\frac{\partial\varphi}{\partial u_0}(t,x_0,u_0)+F_u\frac{\partial u}{\partial u_0} \tag{21}$$

Here, F_x, F_u can be calculated as follows:

$$F_x=\frac{\partial f}{\partial x}(\varphi(t,x_0,u_0),u)\,,$$
$$F_u=\frac{\partial f}{\partial u}(\varphi(t,x_0,u_0),u)\,. \tag{22}$$

Moreover, by introducing the variable, τ, which is called Control Period here, and defining u_0 as the control input to the system during $(t_0, t_0+\tau)$ while $x = x_0$, the input torque u can be described in Eq. (23).

$$u=\mathrm{rect}(t)u_0, \tag{23}$$

where $\mathrm{rect}(t)$ is a rectangular function defined as follows:

$$\mathrm{rect}(t)=\begin{cases}1, & \text{if } (kT+t_0)<t\le(kT+t_0+\tau)\\ 0 & \text{otherwise}\end{cases}$$

Here, $k = (0, 1, 2, \ldots)$, and t_0 is the time at the Poincaré section.

From Eqs. (20)–(22), each matrix of A and B can be calculated by carrying out integrals in numerical integration to the above fundamental matrix solution of linear differential equations over the interval, $t \in [0, T]$.

4.2.2 Stability analysis

Since the value of both the matrix A and the matrix B can be calculated, i.e., the stabilization problem of the 3-link gymnastic robot can be reduced to that of a discrete model described in Eq. (16). For investigating the stabilization of gymnastic robot's continuous-time system by dynamic delayed feedback control, it is sufficient to consider the discrete-time model.

Here, a modified dynamic DFC controller to stabilize the system (8) is adopted as follows:

$$\left.\begin{aligned}\hat{x}(k+1)&=\hat{A}\hat{x}(k)+\hat{B}y(k),\\ u(k)&=\hat{C}\hat{x}(k)+\hat{D}y(k),\\ y(k)&=\mu(\mathrm{x}(k)-\mathrm{x}(k-1))\\ &\equiv\mu(x(k)-x(k-1)),\end{aligned}\right\} \tag{24}$$

where $\hat{A}\in\Re^{\hat{n}\times\hat{n}}$, $\hat{B}\in\Re^{\hat{n}\times n}$, $\hat{C}\in\Re^{m\times\hat{n}}$, $\hat{D}\in\Re^{m\times n}$, $\hat{x}\in\Re^{\hat{n}}$. Here, $\hat{x}$ is the state of the controller, $\mathrm{x}(k)$ denotes the state which is the kth intersection point of unstable periodic orbit and Poincaré map, P. The control input $u(k)$ is applied to (8) only if $\|y(k)\| < \varepsilon$, otherwise $u(k) = 0$ and $\hat{x}(k) = 0$. ε is a given sufficient small positive number. In addition, by means of numerical analysis, it was found that the sign of $x(k)-x(k-1)$ seems to be able to affect the dynamics of the controlled system. Therefore, a variable μ, whose value is (1,or,-1), is introduced as a design parameter.

The linearized closed-loop system with the extended dynamic DFC (24) can be described by

$$x_c(k+1)=A_cx_c(k), \tag{25}$$

where

$$A_c=\begin{bmatrix}A+\mu B\hat{D} & -\mu B\hat{D} & B\hat{C}\\ I_n & 0 & 0\\ \mu\hat{B} & -\mu\hat{B} & \hat{A}\end{bmatrix},$$
$$x_c(k)=\begin{bmatrix}x(k)\\ x(k-1)\\ \hat{x}(k)\end{bmatrix}. \tag{26}$$

Thus, the local stability of the system (16) with the controller (24) is reduced to that of (25). Here, it is considered only the case of $\hat{n} = n$. Then, a controller having the coefficient is given as follows:

$$\left.\begin{aligned}\hat{A}&=(I_n-A)^{-1}BK,\\ \hat{B}&=-(I_n-A)^{-1}BKA(I_n-A)^{-1},\\ \hat{C}&=K,\\ \hat{D}&=-KA(I_n-A)^{-1},\end{aligned}\right\} \tag{27}$$

where K is a gain matrix.

Therefore, a theorem is obtained as follows:

Theorem 1 *Assume that (A, B) is stabilizable. Then, there exists an nth-order dynamic delayed feedback controller (24),(27) such that the closed-loop system (25) is asymptotically stable if and only if $I_n - \mu A$ is nonsingular and $A + BK(I_n - \mu A)(I_n - A)^{-1}$ is asymptotically stable.*

Proof Introducing a matrix as follows:

$$Q = \begin{bmatrix} I_n & 0 & 0 \\ 0 & I_n & 0 \\ (I_n - A)^{-1} & -A(I_n - A)^{-1} & -I_n \end{bmatrix}, \quad (28)$$

it is obvious that

$$Q = Q^{-1}.$$

Then, using a similarity transformation of A_c by the matrix Q, it obtained the Eq. (29).

Consider each matrix of $\hat{A}, \hat{B}, \hat{D}$ as a matrix function of the matrix $\hat{C}$. Then, a solution of Eqs. (30)–(32) is obtained as follows:

$$\left.\begin{aligned} \hat{A} &= (I_n - A)^{-1} B\hat{C}, \\ \hat{B} &= -(I_n - A)^{-1} B\hat{C} A (I_n - A)^{-1}, \\ \hat{D} &= -\hat{C} A (I_n - A)^{-1}. \end{aligned}\right\} \quad (36)$$

If let $\hat{C} = K$, it is obvious that Eq. (36) is equivalent to Eq. (27). Thus, Eq. (29) is reduced to be

$$\begin{aligned} Q^{-1} A_c Q &= \begin{bmatrix} I_n & 0 & 0 \\ 0 & I_n & 0 \\ (I_n - A)^{-1} & -A(I_n - A)^{-1} & -I_n \end{bmatrix} \begin{bmatrix} A + \mu B\hat{D} & -\mu B\hat{D} & B\hat{C} \\ I_n & 0 & 0 \\ \mu\hat{B} & -\mu\hat{B} & \hat{A} \end{bmatrix} Q, \\ &= \begin{bmatrix} A + \mu B\hat{D} & -\mu B\hat{D} & B\hat{C} \\ I_n & 0 & 0 \\ (I_n - A)^{-1}(A + \mu B\hat{D}) - A(I_n - A)^{-1} - \mu\hat{B} & -(I_n - A)^{-1} \cdot \mu B\hat{D} + \mu\hat{B} & (I_n - A)^{-1} B\hat{C} - \hat{A} \end{bmatrix} \\ &\quad \cdot \begin{bmatrix} I_n & 0 & 0 \\ 0 & I_n & 0 \\ (I_n - A)^{-1} & -A(I_n - A)^{-1} & -I_n \end{bmatrix} \\ &= \begin{bmatrix} A + \mu B\hat{D} + B\hat{C}(I_n - A)^{-1} & -\mu B\hat{D} - B\hat{C}A(I_n - A)^{-1} & -B\hat{C} \\ I_n & 0 & 0 \\ (I_n - A)^{-1}(A + \mu B\hat{D}) - A(I_n - A)^{-1} - \mu\hat{B} + (I_n - A)^{-1} B\hat{C}(I_n - A)^{-1} - \hat{A}(I_n - A)^{-1} & -(I_n - A)^{-1}\mu B\hat{D} + \mu\hat{B} - (I_n - A)^{-1} B\hat{C}A(I_n - A)^{-1} + \hat{A}A(I_n - A)^{-1} & -(I_n - A)^{-1} \cdot B\hat{C} + \hat{A} \end{bmatrix} \\ &\equiv \tilde{A}_c \end{aligned} \quad (29)$$

To simplify the analysis, it is desired that each item of the third row of the matrix $\tilde{A}_c$ in Eq. (29) equals zero as Eqs. (30)–(32) :

$$(I_n - A)^{-1}(A + \mu B\hat{D}) - A(I_n - A)^{-1} - \mu\hat{B} + (I_n - A)^{-1} B\hat{C}(I_n - A)^{-1} - \hat{A}(I_n - A)^{-1} = 0, \quad (30)$$

$$-(I_n - A)^{-1}\mu B\hat{D} - (I_n - A)^{-1} B\hat{C}A(I_n - A)^{-1} + \mu\hat{B} + \hat{A}A(I_n - A)^{-1} = 0, \quad (31)$$

$$-(I_n - A)^{-1} B\hat{C} + \hat{A} = 0. \quad (32)$$

Note equality holds in the following equation.

$$(I_n - A)^{-1} A = A(I_n - A)^{-1} \quad (33)$$

From Eqs. (32) and (33), one can simplify Eqs. (30) and (31) to be a same equality as follows:

$$(I_n - A)^{-1}\mu B\hat{D} - \mu\hat{B} = 0. \quad (34)$$

With reference to the item in the first row and the second column of the matrix $\tilde{A}_c$, $\hat{D}$ can be chosen as follows:

$$\hat{D} = -\hat{C}A(I_n - A)^{-1}. \quad (35)$$

$$Q^{-1} A_c Q = \begin{bmatrix} A + BK(I_n - \mu A)(I_n - A)^{-1} & (*) & -BK \\ I_n & 0 & 0 \\ 0 & 0 & 0 \end{bmatrix},$$

which is stable if and only if $A + BK(I_n - \mu A)(I_n - A)^{-1}$ is asymptotically stable. □

Furthermore, if let $\hat{K} = K(I_n - \mu A)(I_n - A)^{-1}$, the stabilization problem of the closed-loop system becomes a problem as follows:

Problem 1 Given a system (25), find a feedback gain $\hat{K}$ that places the closed-loop poles of the system in the set $\Gamma = \{z \in \mathrm{C} : |z| < 1\}$.

As is well known, $\hat{K}$ is a solution of Problem 1 if and only if the matrix $A + B\hat{K}$ has its eigenvalues in the above set of Γ. Hence, it is not difficult to obtain the value of $\hat{K}$ by using the pole placement technique. If $\det(I_n - \mu A) \cdot \det(I_n - A)^{-1} \neq 0$, then the feedback gain K is given by

$$K = \hat{K}(I_n - A)(I_n - \mu A)^{-1}. \quad (37)$$

Table 2 Control parameters (GRM-I)

Case	Initial condition	Pole of the linearized closed-loop system	μ	ε
I	$(-\pi, 0.1, 0.2, 6.683, 0.222, 3.183)$	(0.88+0.1i, 0.88−0.1i, 0.89+0.1i, 0.89−0.1i, 0.9+0.1i, 0.9−0.1i)	1	2
II	$(-\pi, 0.05, 0.05, 0.863, 19.292, -18.25)$	(0.2+0.05i, 0.2−0.05i, 0.25+0.05i, 0.25−0.05i, 0.3+0.05i, 0.3−0.05i)	−1	5

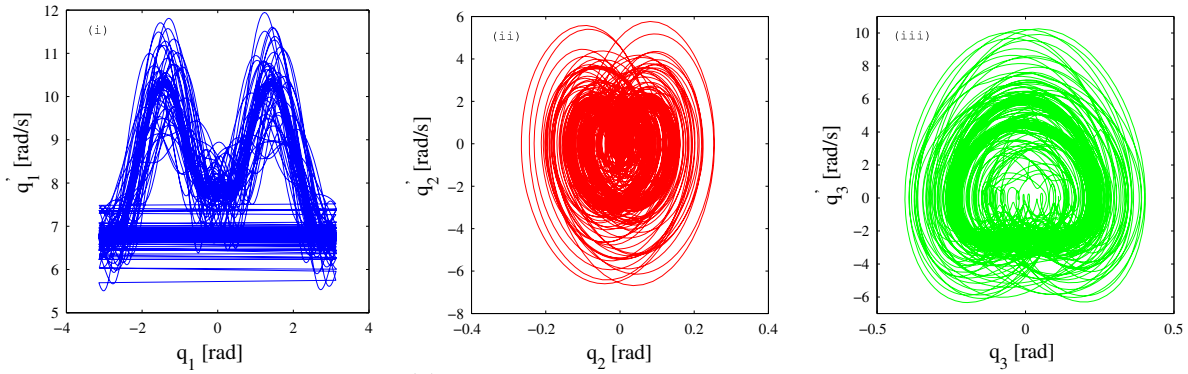

(a) Phase portrait of $q - \dot{q}$ ($t = 0 \sim 80$[s])

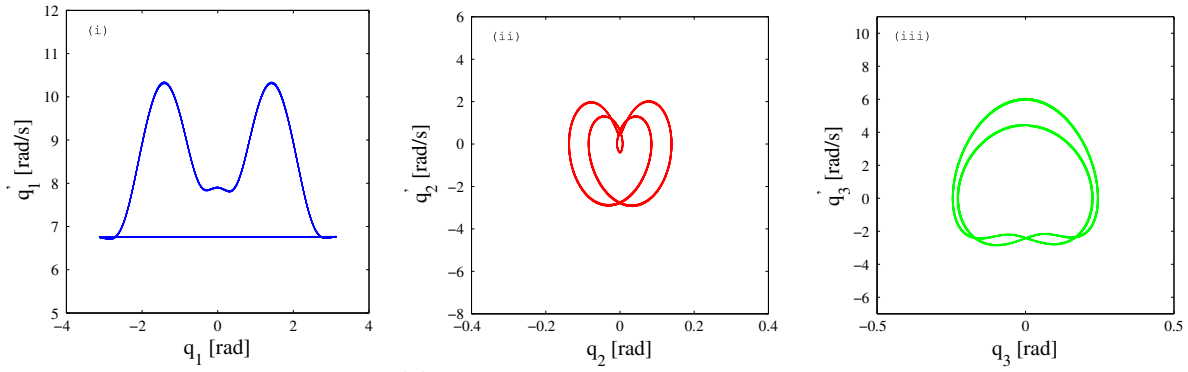

(b) Phase portrait of $q - \dot{q}$ ($t = 80 \sim 100$[s])

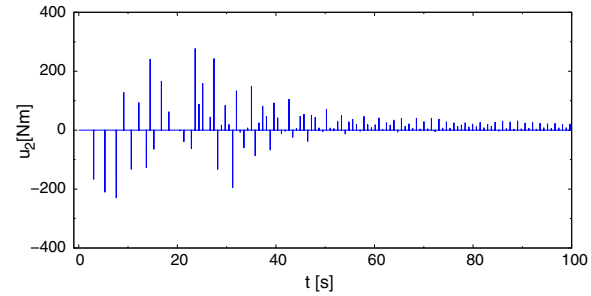

(c) Control input u_2

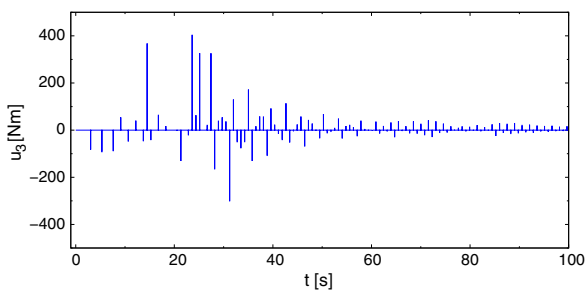

(d) Control input u_3

Fig. 3 Stabilizing case-I orbits: **a** phase portrait with $t = 0$–80 s; **b** phase portrait with $t = 80$–100 s; **c** time history of control input u_2; **d** time history of control input u_3. (GRM-I)

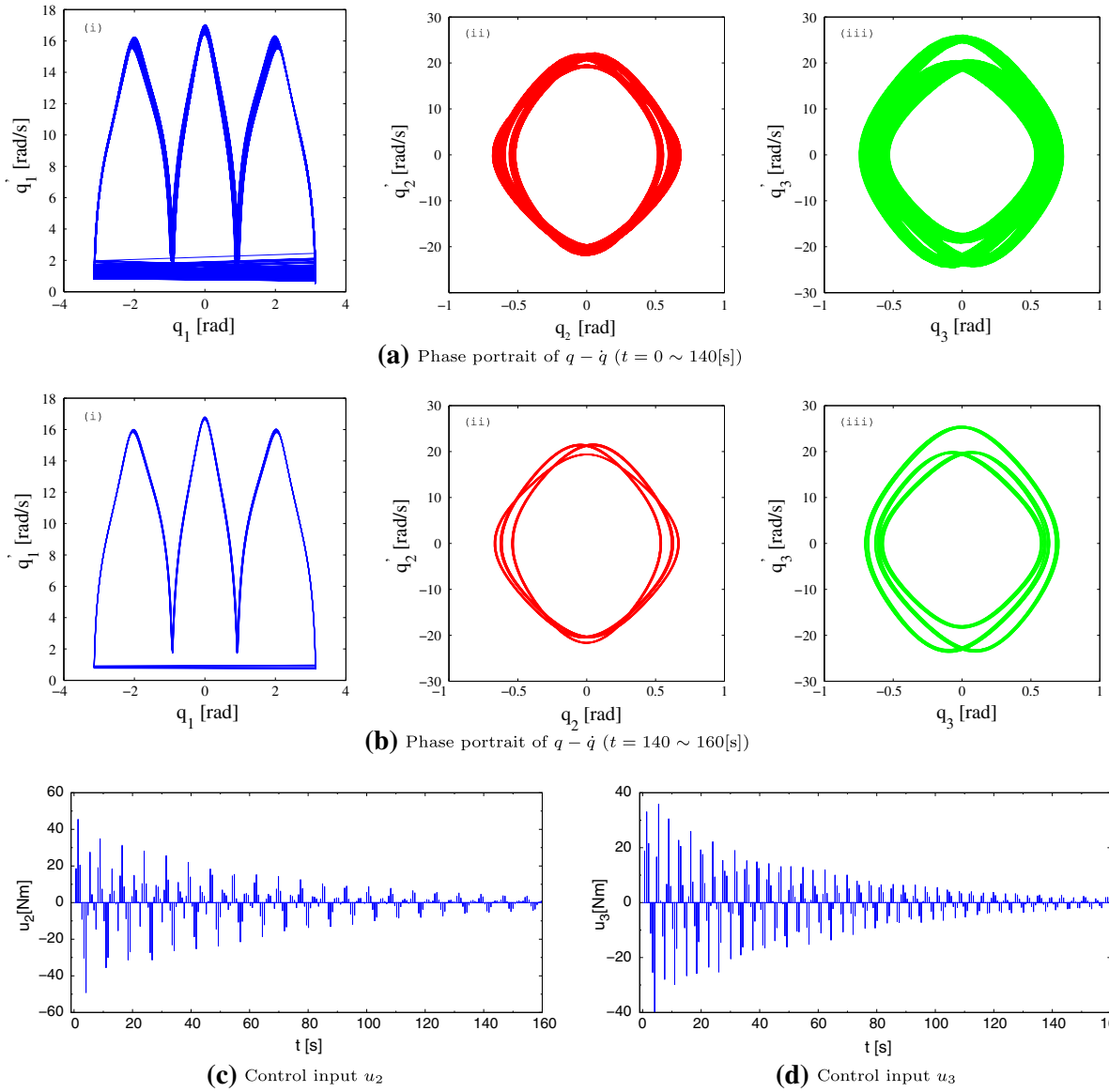

Fig. 4 Stabilizing case-II orbits: **a** phase portrait with $t = 0$–$140\,\mathrm{s}$; **b** phase portrait with $t = 140$–$160\,\mathrm{s}$; **c** time history of control input u_2; **d** time history of control input u_3. (GRM-I)

5 Numerical simulations

This section presents some simulation results to verify the validity of the proposed method for controlling the giant swing motions of the gymnastic robot. Two gymnastic robot with different model parameters are examined by means of the proposed method. In solving the differential equations, 4th-order Runge–Kutta method was used with time step size $\mathrm{d}t = 1\,\mathrm{ms}$. The control period τ is set to 5 ms.

5.1 Gymnastic robot model I (GRM-I)

In this subsection, the parameters of the gymnastic robot model are used as shown in Table 1. Here, two

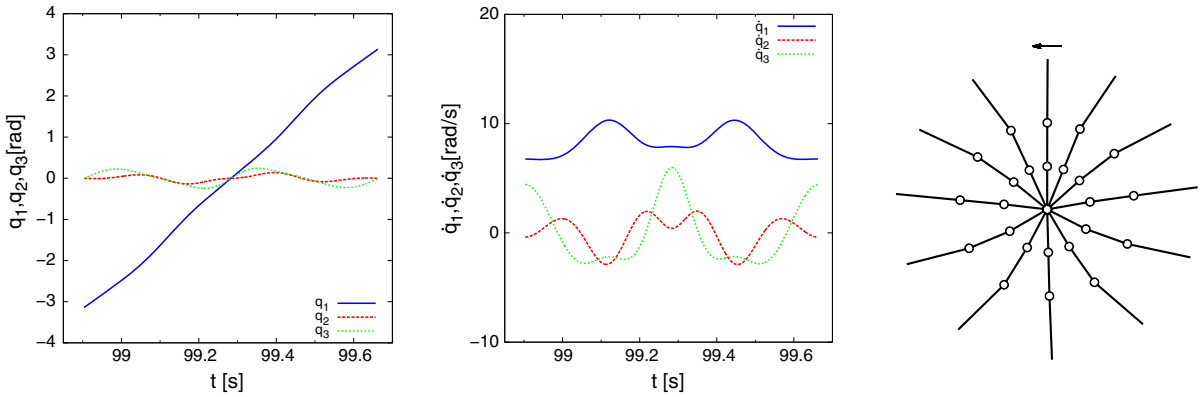

(a) Angular **(b)** Angular velocity **(c)** Stick

Fig. 5 Angle, angular velocity, and stick diagram while the system succeed to form a stable giant swing motion in case-I. (GRM-1)

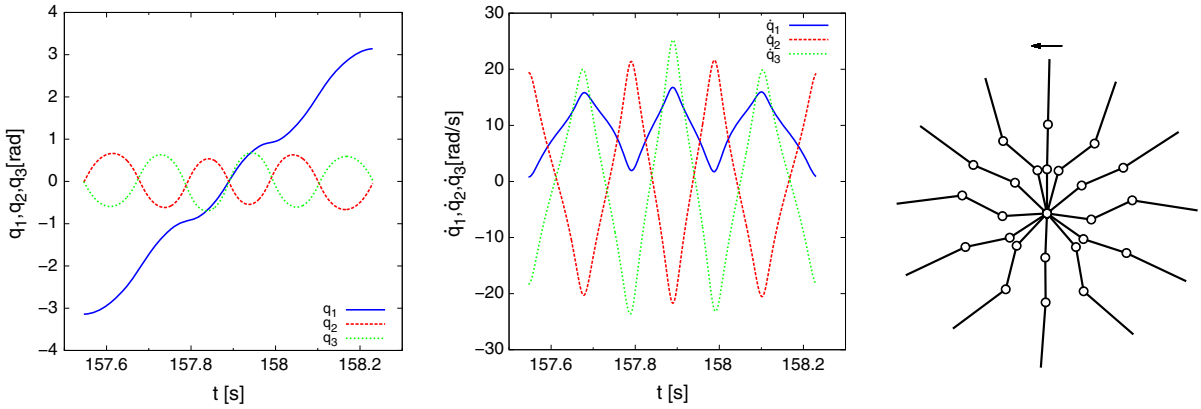

(a) Angular **(b)** Angular velocity **(c)** Stick

Fig. 6 Angle, Angular velocity and Stick diagram while the system succeed to form a stable giant swing motion in case-II. (GRM-I)

cases shown in Table 2, in which the system starts its movement from different initial conditions, were studied below. From Fig. 2b and d, it has been known that the dynamics of the system was chaotic without the control input u.

Using the method discussed in Sect. 4.2.1, the error transfer matrix A and the input matrix B of these two cases can be computed, respectively, in which two unstable fixed points of the system used as the initial conditions were set as the following cases:

$$\begin{cases} \text{I} & : (-\pi, 0, 0, 7.483, -0.278, 4.383) \\ \text{II} & : (-\pi, 0, 0, 0.763, 18.886, -17.648) \end{cases} \tag{38}$$

Then, by assigning, respectively, the poles of $A + BK(I_n - \mu A)(I_n - A)^{-1}$ in the unit disk, as shown in Table 2, the gain matrix K can be obtained. From Eq. (27), each $\hat{A}$, $\hat{B}$, $\hat{C}$, $\hat{D}$ could be calculated using the obtained values of A, B, and K. Thus, an extended dynamic delayed feedback controller could be designed to control the dynamics of the system.

Table 3 Link parameter values [45]

	1st link	2nd link	3rd link
Mass m_i (kg)	5.4	29.5	18.5
Moment of inertia I_i (kgm^2)	0.15	1.93	1.03
Link length l_i (m)	0.58	0.50	0.79
Offset of mass center a_i (m)	0.31	0.20	0.33

The numerical simulation results are shown in Figs. 3 and 4, in which Fig. 3 shows the results of case-I, while Fig. 4 displays that of case-II. Meanwhile, Figs. 3a, b, and 4a, 4b plot the trajectory of the orbits in the phase plane $(q, \dot{q})$, which refer to, respectively, the angle, angular velocity of the link. The time histories

Table 4 Control parameters (GRM-II)

Initial condition	Pole of the linearized closed-loop system	μ	ε
$(-\pi, 0.1, 0.1, 4.225, 9.30, -6.29)$	(0.81+0.1i, 0.81−0.1i, 0.83+0.1i, 0.83−0.1i, 0.85+0.1i, 0.85−0.1i)	1	1.5

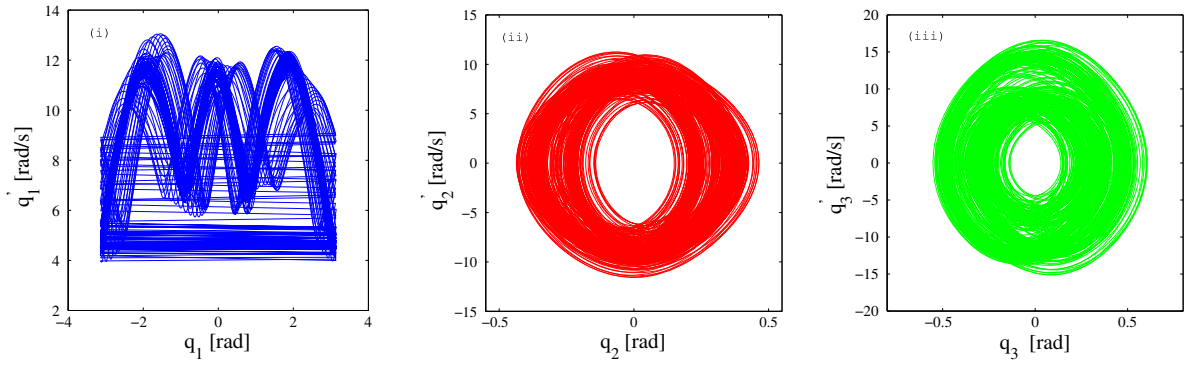

(a) Phase portrait of $q - \dot{q}$ $(t = 0 \sim 100[\mathrm{s}])$

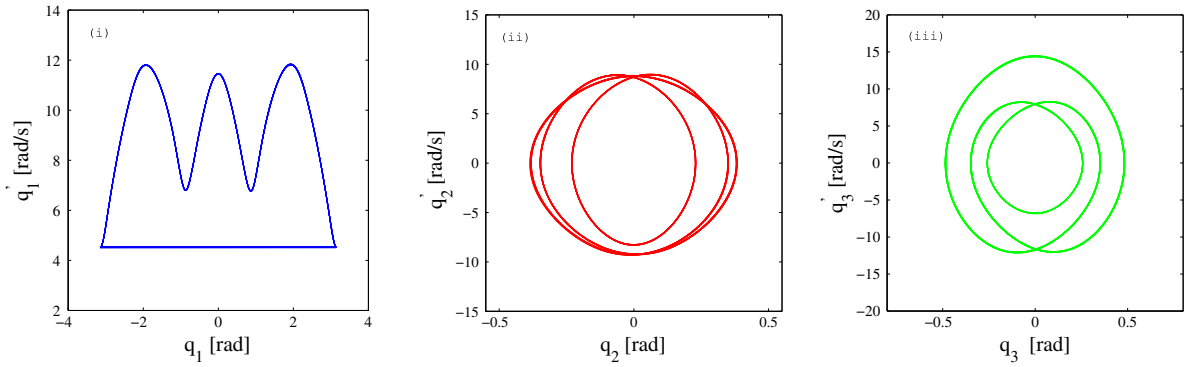

(b) Phase portrait of $q - \dot{q}$ $(t = 100 \sim 120[\mathrm{s}])$

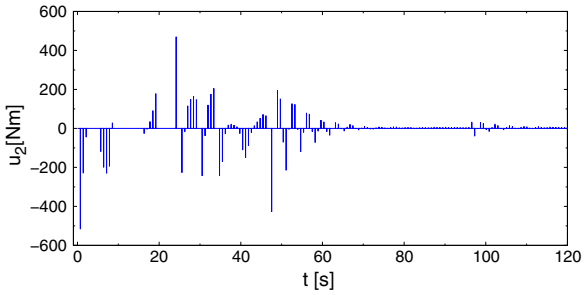

(c) Control input u_2

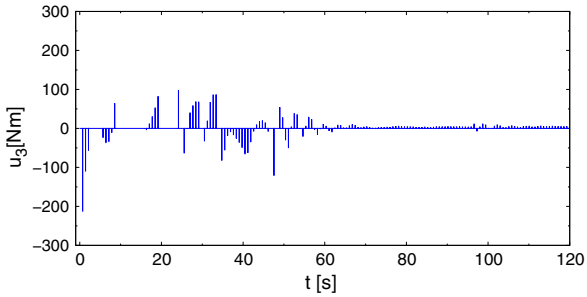

(d) Control input u_3

Fig. 7 Stabilizing orbits: **a** phase portrait with $t = 0$–100 s; **b** phase portrait with $t = 100$–120 s; **c** time history of control input u_2; **d** time history of control input u_3. (GRM-II)

of control input were depicted in Figs. 3c, 3d, and 4c, d, respectively.

In addition, Figs. 5 and 6 depict, respectively, the angle, angular velocity, and stick diagrams based on one period data after the giant swing motion converging to a stable periodic orbit. In the above two cases, each one of the intersection point of the periodic orbit and the Poincaré map converges to a fixed point as follows:

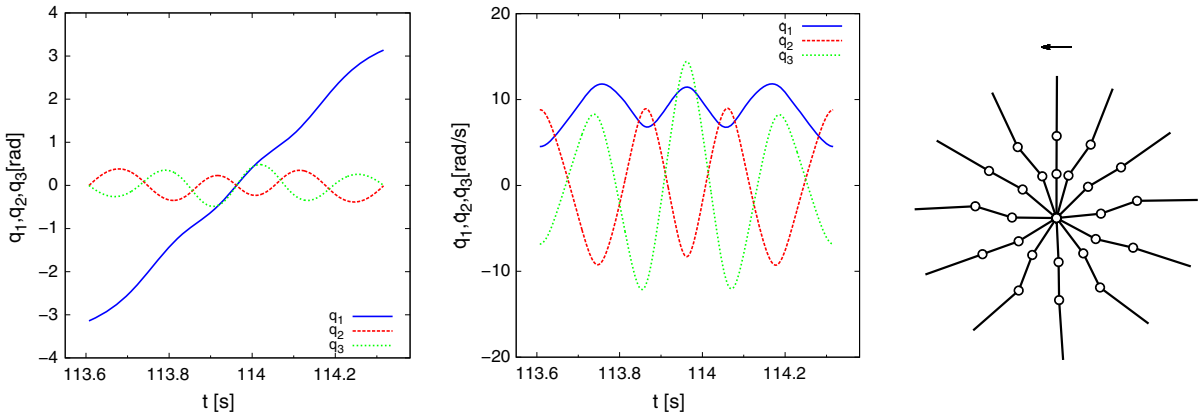

(a) Angular **(b)** Angular velocity **(c)** Stick

Fig. 8 Angle, angular velocity and stick diagram while the system succeed to form a stable giant swing motion. (GRM-II)

$$\begin{cases} \text{I} & : (-\pi, -0.001, -0.005, 6.767, -0.410, 4.455) \\ \text{II} & : (-\pi, -0.020, -0.004, 0.818, 19.375, -18.292) \end{cases} \quad (39)$$

Compare Eq. (38) with Eq. (39), one will find a little difference between them. This difference is thought to be caused by the error between the continuous-time system of the 3-link gymnastic robot and its discretization model. Nevertheless, for a gymnastic robot system, periodicity is more important relative to the exact fixed point.

It can be known from these simulation results that the controlled system succeeded to form two kinds of giant swing motions from the suspended posture by using the dynamic delayed feedback control method.

5.2 Gymnastic robot model II (GRM-II)

To confirm whether the proposed method is effective while being applied to a gymnastic robot with different parameters, in this subsection, an examination was conducted to a different gymnastic robot model whose parameters shown in Table 3 are the same as those presented in the reference [45].

Similar to Sect. 5.1, the error transfer matrix A and the input matrix B can be computed, in which an unstable fixed point of the system used as the initial conditions was set to be $(-\pi, 0, 0, 4.525, 8.846, -6.791)$. Then, by assigning the poles of $A + BK(I_n - \mu A)(I_n - A)^{-1}$ in the unit disk, as shown in Table 4, the gain matrix K can be obtained. From Eq. (27), each $\hat{A}, \hat{B}, \hat{C}, \hat{D}$ could be calculated similarly using the obtained values of A, B, and K. Thus, an extended dynamic delayed feedback controller could be designed.

The numerical simulation results are shown in Figs. 7 and 8, in which Fig. 7 plots the trajectory of the orbits in the phase plane $(q, \dot{q})$, which refer to respectively the angle, angular velocity of the link, and the time history of control input, Fig. 8 depicts the angle, angular velocity, and stick diagrams based on one period data after the giant swing motion converging to a stable periodic orbit. The intersection point of the periodic orbit and the Poincaré map converges to a fixed point as $(-\pi, -0.003, -0.002, 4.530, 8.811, -6.827)$.

From the above simulation results, it can be seen that the proposed method is also effective in controlling a gymnastic robot with different model parameters to perform a stable periodic giant swing motion.

6 Conclusion

This paper studied the behavior of the giant swing motions of a 3-link gymnastic robot by means of the dynamic delayed feedback control. Firstly, a mode of a 3-link gymnastic robot was given and its periodic and chaotic motions were presented by numerical simulations. Secondly, a method of the extended dynamic delayed feedback control, which is an extension of the original dynamic DFC, was proposed. Meanwhile, a discretization way to calculate the error transfer matrix and the input matrix was discussed. Finally, the simulation results showed its effectiveness via the proposed method.

Acknowledgments This work is supported in part by the Project Sponsored by the Scientific Research Foundation for the Returned Overseas Chinese Scholars, State Education Ministry, and in part by the Scientific Research Foundation for Young Teachers, Shanghai JiaoTong University. The authors thank the anonymous reviewers for their useful comments and suggestions.

References

1. Spong, M.W.: The swing up control problem for the actobot. IEEE Control Syst. **15**, 49–55 (1995)
2. Michitsuji, Y., Sato, H., Yamakita, M.: Giant swing via forward upward circling of the acrobat-robot. Proc. Am. Control Conf. **4**, 3262–3267 (2001)
3. Ono, K., Yamamoto, K., Imadu, A.: Control of giant swing motion of a two-link horizontal bar gymnastic robot. Adv. Robot. **15**(4), 449–465 (2001)
4. Yamaura, H., Yanai, M.: A realization method of giant-swing motion of 3-dof link mechanism. Trans. Jpn. Soc. Mech. Eng. **72–721**, 2812–2820 (2006). (in Japanese)
5. Xin, X., She, J.H., Yamasaki, T., Liu, Y.: Swing-up control based on virtual composite links for-link underactuated robot with passive first joint. Automatica **45**(9), 1986–1994 (2009)
6. Lai, X.Z., Pan, C.Z., Wu, M., Yang, S.X.: Unified control of n-link underactuated manipulator with single passive joint: a reduced order approach. Mech. Mach. Theory **56**, 170–185 (2012)
7. Yamasaki, T., Gotoh, K., Xin, X.: Optimality of a kip performance on the high bar: an example of skilled goal-directed whole-body movement. Hum. Mov. Sci. **29**(3), 464–482 (2010)
8. Lai, X., Zhang, A., Wu, M., She, J.: Singularity-avoiding swing-up control for underactuated three-link gymnast robot using virtual coupling between control torques. Int. J. Robust Nonlinear Control (2013). doi:10.1002/nc.3082
9. Eldukhri, E., Kamil, H.: Optimisation of swing-up control parameters for a robot gymnast using the bees algorithm. J. Intell. Manuf. **235**, 1–9 (2013)
10. Sano, A.: Dynamic biped walking by using skillfully a gravity field (challenge to a human walking). J. Robot. Soc. Jpn. **11**(3), 52–57 (1993). (in Japanese)
11. Saito, F., Fukuda, T., Arai, F.: Swing and locomotion control for a two-link brachiation robot. IEEE Control Syst. **14**(1), 5–12 (1994)
12. Ott, E., Grebogi, C., Yorke, J.: Controlling chaos. Phys. Rev. Lett. **64**(11), 1196–1199 (1990)
13. Pyragas, K.: Continuous control of chaos by self-controlling feedback. Phys. Lett. A **170**(6), 421–428 (1992)
14. Socolar, J.E.S., Sukow, D.W., Gauthier, D.J.: Stabilizing unstable periodic orbits in fast dynamical systems. Phys. Rev. E **50**, 3245–3248 (1994)
15. Vasegh, N., Sedigh, A.K.: Delayed feedback control of time-delayed chaotic systems: analytical approach at hopf bifurcation. Phys. Lett. A **372**(31), 5110–5114 (2008)
16. Fuh, C.C., Tung, P.C.: Robust control for a class of nonlinear oscillators with chaotic attractors. Phys. Lett. A **218**(3–6), 240–248 (1996)
17. Sinha, S., Ramaswamy, R., Rao, J.: Adaptive control in nonlinear dynamics. Phys. D **43**(1), 118–128 (1990)
18. Wang, X., Wang, Y.: Adaptive control for synchronization of a four-dimensional chaotic system via a single variable. Nonlinear Dyn. **65**, 311–316 (2011)
19. Nazzal, J.M., Natsheh, A.N.: Chaos control using sliding-mode theory. Chaos Solitons Fractals **33**(2), 695–702 (2007)
20. Salarieh, H., Alasty, A.: Control of stochastic chaos using sliding mode method. J. Comput. Appl. Math. **225**(1), 135–145 (2009)
21. Layeghi, H., Arjmand, M.T., Salarieh, H., Alasty, A.: Stabilizing periodic orbits of chaotic systems using fuzzy adaptive sliding mode control. Chaos Solitons Fractals **37**(4), 1125–1135 (2008)
22. Li, G.H., Zhou, S.P., Yang, K.: Generalized projective synchronization between two different chaotic systems using active backstepping control. Phys. Lett. A **355**(45), 326–330 (2006)
23. Huang, T., Li, C., Yu, W., Chen, G.: Synchronization of delayed chaotic systems with parameter mismatches by using intermittent linear state feedback. Nonlinearity **22**, 569–584 (2009)
24. Gan, Q.: Exponential synchronization of stochastic cohen-grossberg neural networks with mixed time-varying delays and reactiondiffusion via periodically intermittent control. Neural Netw. **31**, 12–21 (2012)
25. Ushio, T.: Limitation of delayed feedback control in nonlinear discrete-time systems. IEEE Trans. Circuits Syst. I **43**(9), 815–816 (1996)
26. Just, W., Bernard, T., Ostheimer, M., Reibold, E., Benner, H.: Mechanism of time-delayed feedback control. Phys. Rev. Lett. **78**(2), 203–206 (1997)
27. Nakajima, H.: On analytical properties of delayed feedback control of chaos. Phys. Lett. A **232**(3–4), 207–210 (1997)
28. Yamamoto, S., Hino, T., Ushio, T.: Dynamic delayed feedback controllers for chaotic discrete-time systems. IEEE Trans. Circuits Syst. I **48**(6), 785–789 (2001)
29. Pyragas, K.: Control of chaos via extended delay feedback. Phys. Lett. A **206**(5–6), 323–330 (1995)
30. Bleich, M.E., Socolar, J.E.S.: Stability of periodic orbits controlled by time-delay feedback. Phys. Lett. A **210**(1–2), 87–94 (1996)
31. Ushio, T., Yamamoto, S.: Prediction-based control of chaos. Phys. Lett. A **264**(1), 30–35 (1999)
32. Just, W., Popovich, S., Amann, A., Baba, N., Schöll, E.: Improvement of time-delayed feedback control by periodic modulation: analytical theory of floquet mode control scheme. Phys. Rev. E **67**(2), 026 (2003). 222
33. ZUO, W., WEI, J.: Stability and bifurcation analysis in a diffusive brusselator system with delayed feedback control. Int. J. Bifurc. Chaos **22**(02), 1250 (2012). 037
34. Botmart, T., Niamsup, P., Liu, X.: Synchronization of non-autonomous chaotic systems with time-varying delay via delayed feedback control. Commun. Nonlinear Sci. Numer. Simul. **17**(4), 1894–1907 (2012)
35. Gjurchinovski, A., Jüngling, T., Urumov, V., Schöll, E.: Delayed feedback control of unstable steady states with high-frequency modulation of the delay. Phys. Rev. E **88**, 032 (2013). 912
36. Pyragas, K., Novičenko, V.: Time-delayed feedback control design beyond the odd-number limitation. Phys. Rev. E **88**, 012 (2013). 903

37. Tweten, D., Mann, B.: Delayed feedback control of chaos for arbitrary delays analyzed with the spectral element method. Int. J. Dyn. Control **1**(4), 283–289 (2013)
38. Jungers, M., Castelan, E.B., Moraes, V.M., Moreno, U.F.: A dynamic output feedback controller for NCS based on delay estimates. Automatica **49**(3), 788–792 (2013)
39. Liu, D., Yamaura, H.: Realization of giant swing motions of a two-link horizontal bar gymnastic robot using delayed feedback control [in japanese]. Trans. Jpn. Soc. Mech. Eng. C **76**(767), 1700–1707 (2010)
40. Liu, D., Yamaura, H.: Stabilization control for giant swing motions of 3-link horizontal bar gymnastic robot using multiple-prediction delayed feedback control with a periodic gain. J. Syst. Des. Dyn. **5**(1), 42–54 (2011)
41. Liu, D., Yamaura, H.: Giant swing motion control of 3-link gymnastic robot with friction around an underactuated joint. J. Syst. Des. Dyn. **5**(5), 925–936 (2011)
42. Ono, K., Imadu, A., Sakai, T.: Optimal motion trajectory of giant swing [in japanese]. Trans. Jpn. Soc. Mech. Eng. C **62**(599), 2640–2647 (1996)
43. Hiroshi, Y., Kyosuke, O., Hiroyuki, S.: Giant-swing motions of a 3-dof link mechanism (in Japanese). In: Dynamics and Design Conference, The Japan Society of Mechanical Engineers (2002–09-13), p. 150 (2012)
44. Wolf, A., Swift, J.B., Swinney, H.L., Vastano, J.A.: Determining lyapunov exponents from a time series. Phys. D **16**(3), 285–317 (1985)
45. Xin, X., Kaneda, M.: Swing-up control for a 3-dof gymnastic robot with passive first joint: design and analysis. IEEE Trans. Robot. **23**(6), 1277–1285 (2007)